Journal of Power Sources, 25 (1989) 195 - 214

STRUCTURAL ANALYSIS OF ALKALINE FUEL CELL ELECTRODES AND ELECTRODE MATERIALS

KLAUS TOMANTSCHGER

Battery Technologies Inc., 2480 Dunwin Drive, Mississauga, Ont. L5L 1J9 (Canada)

KARL V. KORDESCH

Institute of Inorganic Technology, Technical University Graz, A-8010 Graz (Austria)

(Received August 2, 1988; in revised form November 18, 1988)

Summary

An attempt has been made to characterize gas diffusion electrodes and electrode materials used in alkaline fuel cells. A number of techniques such as intrusion porosimetry, surface area analysis, scanning (SEM) and transmission (TEM) electron microscopy in conjuction with X-ray energy spectroscopy (XES), have been used to determine the relation between structural parameters and electrochemical performance. Intrusion porosimetry was given special attention. Mercury intrusion curves were compared with the intrusion behavior obtained with 12 N KOH electrolyte. It became obvious that the electrode structure consists of two components: a primary (macro) structure providing the skeleton of the electrode and determining the mechanical strength, and the secondary (micro) structure ensuring gas transport. The electrochemical reactions proceed in the boundary between the macro and the microstructure near the outside of the carbon particles where the reactant gas, electrolyte, and electrocatalyst meet in a three zone interface.

1. Introduction

Electrode design

Gas diffusion electrodes used in metal–air batteries, fuel cells, and other electrochemical systems consist of several polytetrafluoroethylene (PTFE) bonded carbon layers. They not only serve as reaction zones for energy conversion, but also provide pores for gas transport and act as a barrier to the electrolyte. Generally, the electrodes employ a multilayer construction to accommodate the different physical and chemical requirements [1].

In a typical three layer design (backing, gas diffusion layer, and the active layer) the backing is placed on to the gas side of the electrode to accommodate the bipolar design. The electrode backing needs to have a high permeability to gases, structural strength, corrosion resistance, and high

0378-7753/89/$3.50

conductivity. Metal screens, Teflonized metal plaques, carbon cloth, carbon paper, and carbon felt find consideration.

The diffusion layer contains gas feed channels supplying the active layer with reactants. To avoid any penetration of the electrolyte into the diffusion layer 25 - 50% PTFE is added to the carbon, ensuring hydrophobicity.

The electrocatalyst layer is less wetproofed than the diffusion layer (5 - 25% PTFE) to ensure partial wetting of the carbon and the electrocatalyst particles. In the catalyst layer, a three-phase reaction zone, where fuel, electrolyte, and carbon supported electrocatalyst meet, is created.

Depending on the type of electrolyte and the operating conditions, concentrations of PTFE and carbon, as well as layer thickness and porosity, may vary. However, in all instances electronic conductivity, ionic transport, and fuel transport to, and from, the reaction sites have to be provided.

Electrode materials

Poly(tetrafluoroethylene) (PTFE)

PTFE is a hydrophobic, chemically stable, plastic material used as a binder for different types of carbon to create a porous electrode structure [2]. In 1955 Du Pont de Nemours made PTFE commercially available under the trademark "Teflon". Its use as hydrophobic binder was first patented in 1960 for use in high temperature cells employing molten alkali electrolyte [3]. Electrodes can be made from two types of PTFE, an aqueous suspension and a dry powder.

Carbon materials [4 - 6]

A variety of different carbon materials find use in gas diffusion electrodes. They include graphites, carbon blacks and carbon substrates.

Graphites. In electrochemical systems natural graphites (*e.g.*, Lonza KS44, BET surface area 9 $m^2 g^{-1}$) and artificial graphites (*e.g.*, Asbury Micro #250, BET surface area 22 $m^2 g^{-1}$) are used. Carbon fibres, cloths, and felts, produced by solid-phase pyrolysis of non-melting polymers, rayon, pitch, etc., are used as substrates for gas–electrode backing materials (current collectors).

Carbon black. Carbon blacks are distinguished by surface area, particle size, oil absorption, volatile content, pH, electrical resistivity, density and extent of graphitization. BET surface areas range between 25 and 2000 $m^2 g^{-1}$. Densities vary from 1.9 g cm^{-3} (lampblack) to below 1.4 g cm^{-3} for gas-activated blacks. The surface area of partially graphitized blacks is high. They possess a large, uniform surface of basal graphite planes, are generally used as adsorbents and, in the case of electrodes, as catalyst carriers. Adsorption (saturation and retention) curves of different chemicals are characteristic. The ohmic resistance values are a function of the degree of graphitization, the moisture content, the degree of compression, and are

influenced by the measurement technique used. Electric conductivities vary from 0.001 to 1 Ω cm (Shawinigan Black: 0.1 Ω cm).

Acetylene black is produced by continuous thermal decomposition of acetylene in an oxygen-lean atmosphere [7]. Particles range from 50 to 2000 Å and are joined in a chain-like fashion. The specific density is 1.95 g cm^{-3}, but the apparent density is only 25 g l^{-1}. It is hydrophobic and therefore the ideal material for diffusion layers [8]. It also finds use as a conductivity additive and catalyst carrier, especially after steam activation, which increases the surface area from about 80 m^2 g^{-1} to 300 m^2 g^{-1}.

Vulcan XC-72R is an extra conductive furnace black produced by Cabot and has been a standard in the plastics and fuel cell industry for many years [9].

Black Pearls 2000 carbon black is a fairly new, highly conductive furnace black available in pelleted form, designed for critical applications demanding excellent electrical conductivity, easy processability, physical property retention, and low moisture absorption. The high electrical conductivity (compared with other blacks) results in lower loadings of Black Pearls 2000 in, for example, conductive plastic materials, than in conventional conductive furnace blacks, to attain a specific level of conductivity. Reduced loadings in plastic systems (bipolar plates for batteries, shielding, etc.) offer greater formulation flexibility and improved compound properties.

Compounds made from Black Pearls 2000 offer significantly improved conductivity *versus* compounds made with equivalent loadings of Vulcan XC-72R. The improvement in conductivity is especially apparent above ambient temperatures, providing a distinct advantage in high temperature applications [10]. The use of Black Pearls 2000 as electrocatalyst support in active layers of gas diffusion electrodes for alkaline fuel cells has shown enhanced performance and lifetime over Vulcan XC 72R carbon [11].

Conductive carbon substrates. Carbon paper, cloth or felt are now tailor-made for use in fuel cells [12 - 14]. The substrates contain no plastic binder after the carbonization. To impart a hydrophobic behavior the substrates are Teflonized prior to application of additional layers [15].

Characterization techniques

To assist intrusion porosimetry, scanning electron microscopy (SEM) was employed for the electrode and electrode foils samples. Pores with diameters greater than 100 μm are beyond the resolution of the porosimeter used. Transmission electron microscopy (TEM) was used for carbon powder and carbon activation studies [8].

Porosimetry

It has been recognized that pores can be conveniently categorized into several size ranges. The Kelvin equation [16] is applicable to pore analysis by adsorption studies, leading to measurements of pore size and pore size distri-

bution, relating the equilibrium vapor pressure of a curved surface, such as that of a liquid in a capillary or pore, to the equilibrium pressure of the same liquid on a plane surface below 1000 Å (1 μm), which corresponds to relative pressures near 0.99. Pores with radii greater than this are labeled "macropores".

Pores in the Kelvin range, from about 15 to 1000 Å (10 μm) have traditionally been called "transitional", and pores of less than about 15 Å "micropores" [17]. "Submicropores" have been postulated for pores below 7 Å [18].

As a result of the high surface tension, γ, of a liquid (defined as the work required to produce one square centimeter of surface), mercury ($\gamma = 470$ (dynes cm^{-1}) does not wet most solid surfaces and must be forced to enter a pore. Washburn showed that the pressure, P, required to force a non-wetting fluid into a capillary of diameter, D, is given by [19]:

$$P = -4\gamma \cos \Theta / D$$

where Θ is the contact angle between the fluid and the liquid.

Mercury intrusion to characterize pore characteristics of materials was first suggested in 1921. Forcing a non-wetting fluid, mercury, under different pressures into a sample, revealed information on the pore structure [20, 21]. By the early 1950s the first prototype for intrusion porosimetry was successfully demonstrated by Winslow while at Union Carbide Corporation's Carbon Division.

Advances in technology have improved the instrumentation for accuracy, speed, and ease of handling. Microprocessor technology has led to complete automation of the process over the past 15 years. Several automated porosimeters have become commercially available in recent years. In the present work a 30 000 p.s.i. automated porosimeter was modified to enable the use of intrusion liquids other than mercury [22].

2. Experimental

Carbon activation

Carbon materials used in fuel cell electrodes are frequently subjected to a pretreatment aimed at removing surface groups which initiate corrosion [6]. Kordesch *et al.* report on the pretreatment of carbon at elevated temperatures. Steam or carbon dioxide act as mild oxidation agents at temperatures around 800 °C, improving the performance and lifetime characteristics of the original carbon material [23]. It has been shown that both gases preferentially attack the unstable portions of the carbon, reducing the surface oxide content [23, 24]. For the gas activation process a steam generator has been installed on a muffle furnace capable of activating carbon batches of up to 250 g (Model S-36525-B Hoskins Furnace Type FD). The activation time is adjusted to achieve the desired weight loss (30% on carbons used in electrode fabrication).

The steam activation removes surface groups that can be oxidized, resulting in a more stable carbon material. This is important in view of long-life electrode performance and open circuit (high voltage) stability [25].

Electrode preparation

The electrode manufacturing process has been described in detail in refs. 8, 25, 26. Carbon cloth (Stackpole Panex PWB-3) is wet-proofed by dipping into a diluted Teflon suspension to a loading of 50% PTFE. The PTFE/carbon layers are prepared by mixing the appropriate amounts of the ingredients in a suspension agent (*e.g.*, a light fraction of petrol). Ground filler particles (ammonium bicarbonate) can be added to adjust the porosity. The mixture is homogenized and, after filtering off the suspension agent, a workable dough is obtained. Thin foils are prepared using cross-rolling techniques. The thicknesses of the foils are adjusted using spacers. Individual layers are cut to size: three foils are assembled into a multilayer electrode and cross-rolled together. The final electrodes are prepared using a press with heating platens (F.S. Carver Inc., 12 ton with heating platens, four column press, Model 2697-12). After pressing (20 kg cm^{-2}), the temperature is slowly increased to 100 °C (decomposition temperature of the ammonium bicarbonate), then to 175 °C (evaporation of the suspension agent), and finally electrodes are sintered under slight pressure at 320 °C for 20 min. In the present work all layers have a thickness of 0.4 mm and three layer electrodes of 1.2 mm. Table 1 shows the composition of the different layers.

Porosimeter operation

A special test cell was built to allow the use of different intrusion liquids, eliminating the possibility of contamination of the instrument. Figure 1 shows the concept. The test cell contains two compartments.

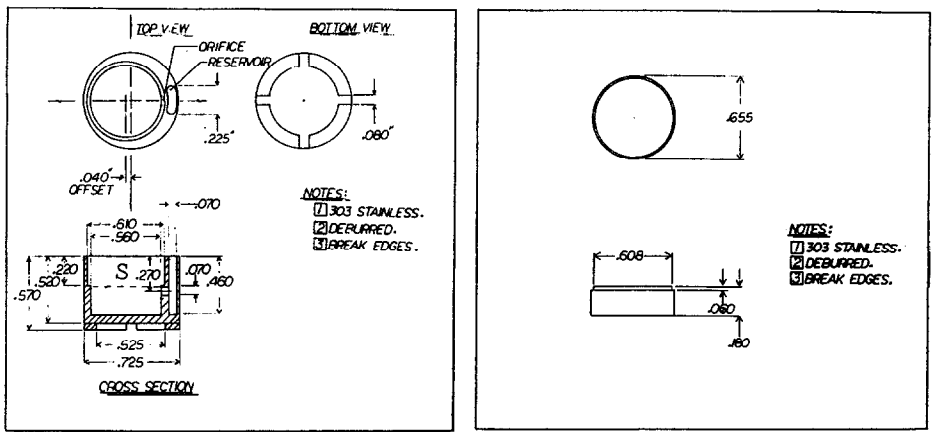

Fig. 1. Porosimeter test cell.

TABLE 1

Electrode foil and electrode compositions including measured and calculated BET surface areas

Element ID	Layer composition (%)		BET Surface areas		
			Components	Calculated	Measured
CC					
Carbon cloth backing	Carbon cloth	50	0.07	6.1	
	PTFE (sus.)	50	6.0		
B902D	SH100	63.5	100.0	65.8	20.0
Cathode diffusion layer	PTFE (Pow.) (filler 60%)	37.5	6.0		
B902C	XC-72R	72	500.0	395.0	120.0
Cathode catalyst layer	10% Pt/XC72R	17	200.0		
	PTFE (Pow.) (filler 15%)	11	6.0		
	0.5 mg Pt cm^{-2}				
B23H2D	BP2000	48	1750.0	845.7	
Anode diffusion layer	Micro # 250	16	22.0		
	PTFE (sus.)	36	6.0		
B23H2C	BP2000	54	1750.0	949.7	728.0
Anode catalyst layer	Micro # 250	13	22.0		
	PTFE (sus.) (postcatalyzed)	31	6.0		

Initially the 750 μl intrusion liquid is placed into the cell. The higher volume compartment contains the sample on a metal screen (electrodes) or a disc (powder samples). After covering, the cell is placed in the sample chamber. During evacuation, the liquid remains in the second compartment, preventing an overflow. In the filling step, the mercury from the reservoir fills the sample chamber. When the mercury enters the sample cell, the intrusion liquid floats on the mercury and is lifted to the sample and starts the intrusion as a function of the applied pressure.

Figure 2 shows the blank volume intrusion curves for mercury and KOH. Both curves are virtually identical. Up to 3000 p.s.i. the curves are very flat, representing the sensitive range of the instrument. At higher pressures some intrusion takes place which is contributed to the reversible deformation of the O-ring seal. The instrument used provides a high resolution in the pore diameter range from 0.1 to 100 μm.

The technique of using mercury and KOH as intrusion liquids for the pore structure of gas diffusion electrodes was first developed by Union Carbide [27]. If the pore size distribution obtained with the actual fuel cell electrolyte is compared with that for mercury, a determination of the wetproofness of the electrode structure can be made.

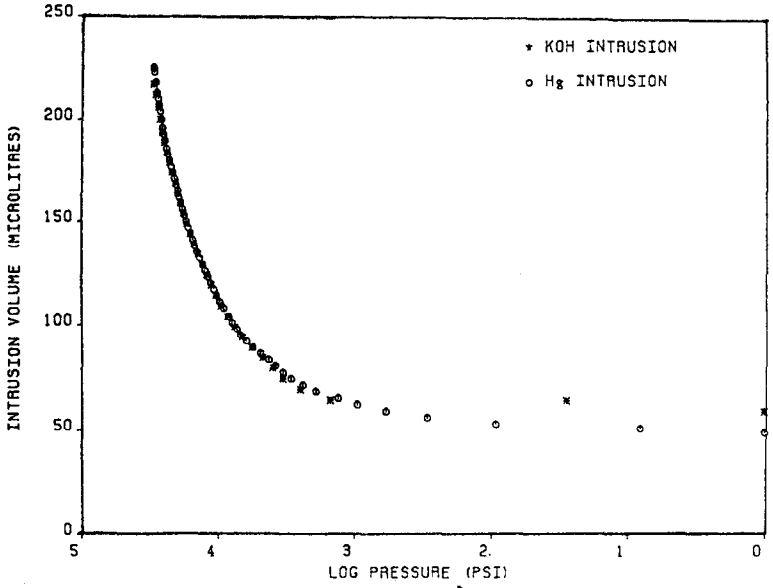

Fig. 2. Blank volume intrusion with mercury and 12 N KOH.

3. Results and discussion

Carbon porosimetry

Porosity data of various graphite and carbon materials were obtained. Hysteresis curves (extrusion) indicate that the intrusion liquid remains in the pores, which is characteristic for ink bottle pores. In pores of this type intrusion cannot occur until sufficient pressure is attained to force mercury into the narrow neck, whereupon the entire pore fills. On depressurization however, the wide pore body will not empty until a lower pressure is reached, and if the neck is sufficiently narrow the mercury may be permanently trapped in the wide part of the pore. Most samples (powder and foils) investigated trapped the intrusion liquid permanently. It is apparant that average pore diameters differ whether they are based on volume, surface area of $4V_{max}/S_{max}$, and further depend on the intrusion pressure range.

The intrusion of mercury and KOH into the pore structure is similar, except that the wetting angle (and therefore the intrusion pressure) for KOH is significantly lower. For this reason, a wetting angle can be determined by forcing a fit between the two distributions.

Figures 3 and 4 show the volume intrusion and intrusion pressures of mercury and 12 N KOH into a graphite rod sample, and Fig. 5 shows the resulting pore size distributions. KOH intrudes the same pores at 1/20 the pressure of mercury. The contact angle used for mercury intrusion is 130° (surface tension: 470 dynes cm^{-1}), the one for 12 N KOH is 100° (surface tension: 85 dynes cm^{-1}). Using matching techniques for the pore size distribution curves, the contact angle of KOH on the graphite rod can be determined as 115°.

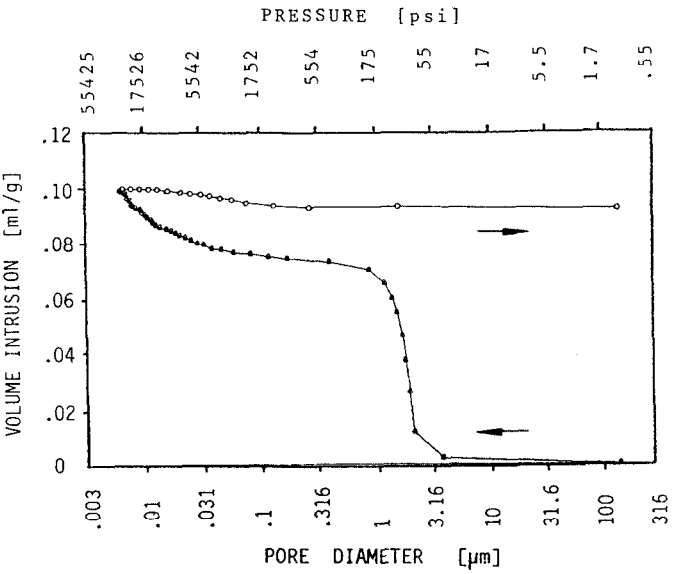

Fig. 3. Mercury volume intrusion and extrusion of a graphite rod.

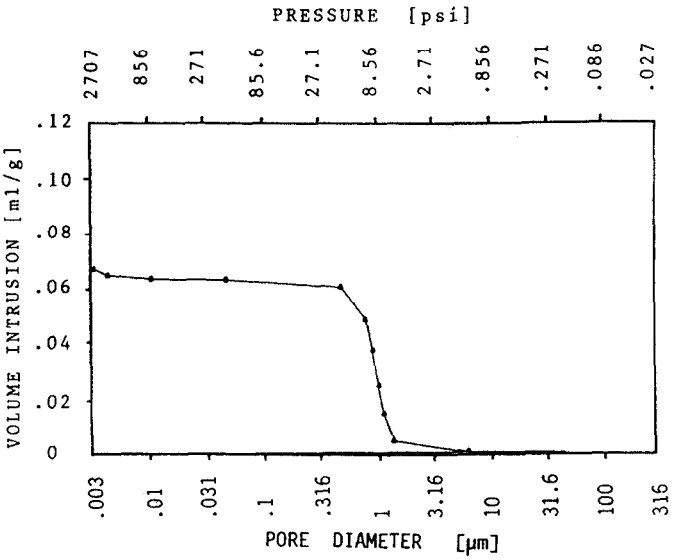

Fig. 4. 12 N KOH volume intrusion of a graphite rod.

Figure 6 shows the pore size distribution curves for Shawinigan SH 100 with Hg and 12 N KOH. The contact angle for KOH (using pore matching) has been determined as 97°.

Figure 7 shows the pore size distribution curves for Vulcan XC 72R with Hg and 12 N KOH. The contact angle for KOH is 101°. Using a contact-anglometer for powder samples the contact angle for mercury on Vulcan XC

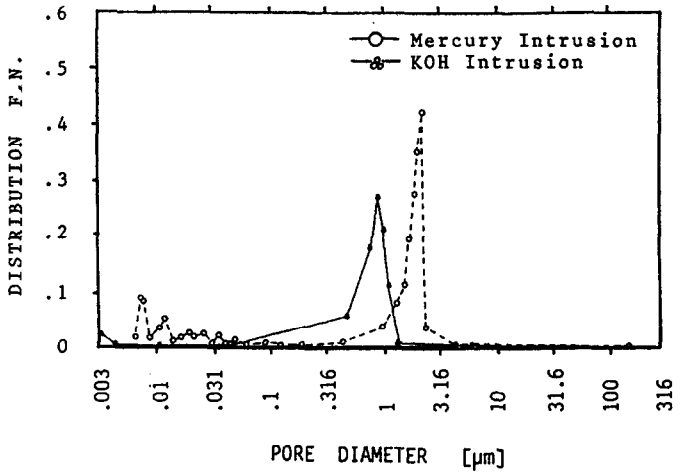

Fig. 5. Pore size distribution for mercury and 12 N KOH intrusion of a graphite rod.

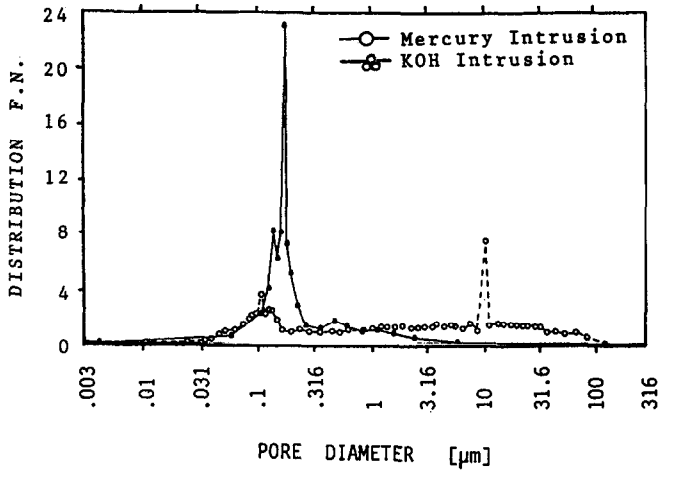

Fig. 6. Pore size distribution for mercury and 12 N KOH intrusion of Shawinigan SH100 acetylene black.

72R was determined as 138°. "Pores" in excess of 1 μm are really interparticle spaces created by the agglomeration of carbon spheres (approx. 0.1 μm dia., see TEM, Fig. 8). These spaces are wetted by KOH and are therefore not apparent in the KOH intrusion curve.

Unactivated carbon powders are virtually hydrophilic, with a wetting angle in KOH of less than 100°. Upon activation, the powders become more hydrophobic, which can contribute to the loss of functional surface groups (—OH, —CHO, —COOH, etc.), with wetting angles approaching 120°.

Upon activation, the apparent density of the carbon powders was seen to decrease. The porosity increases, while the particle size remains practically

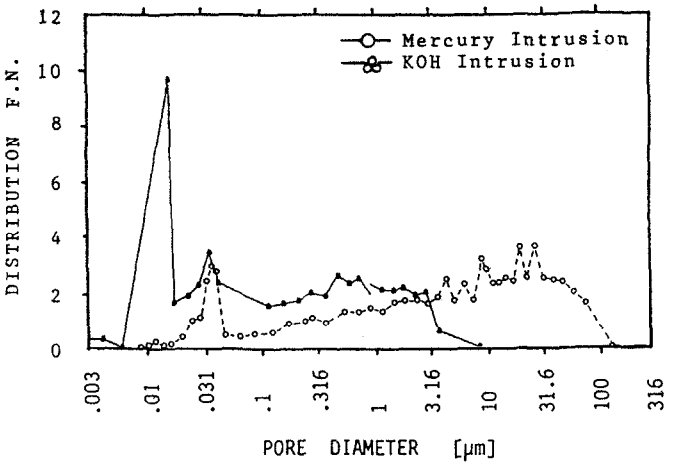

Fig. 7. Pore size distribution for mercury and 12 N KOH intrusion of Vulcan XC 72R.

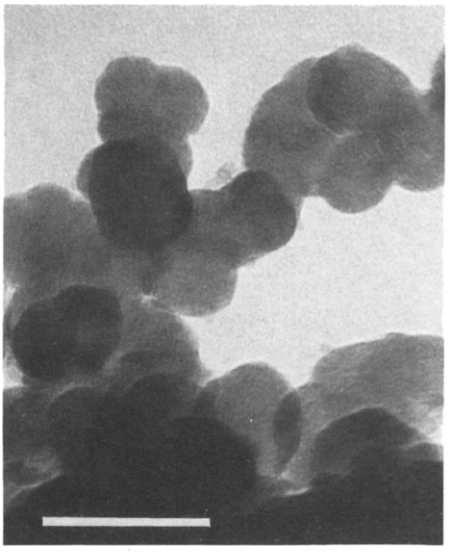

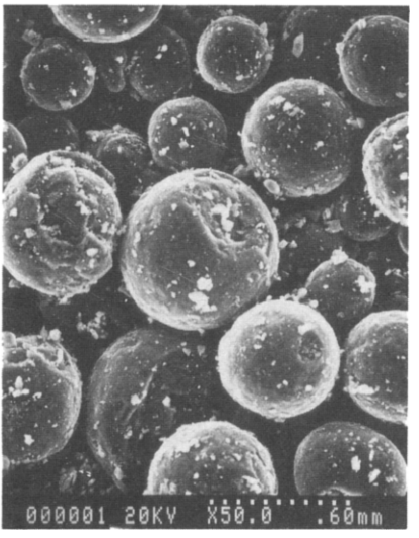

Fig. 8. Transmission electron microscope (TEM) picture of Vulcan XC 72R (Bar = 0.1 μm).

Fig. 9. Scanning electron microscope (SEM) picture of Black Pearls 2000.

unchanged, indicating that (proper) gas activation removes the carbon material inside the particles and (unlike air) does not attack the outside particle which would result in a decrease in particle size [5, 24].

The use of aluminum cobalt (AlCo) spinel, and ruthenium, both enhance the generation of micropore volume during the gas activation and are apparent in the BET surface area, porosity, electrochemical activity, and stability [8].

The AlCo spinel is the important catalyst needed to generate high volume micropores. The addition of spinel was found approximately to double the micropore volume over that obtained when no catalyst was used. The AlCo spinel in the carbon was found to be present in discrete particles averaging about 300 Å in diameter [27].

Black Pearls 2000 consists of spherical carbon agglomerates of 500 μm size (Fig. 9: SEM). Those agglomerates can be dispersed to carbon particles of 0.1 μm size. Pores exist over a wide range of diameters (0.009 - 150 μm).

Electrode structures

Data were obtained for intrusion of the cathode diffusion layer (B902D), the active layer (B902C) and the three layer electrode (containing a carbon cloth backing: B902) (Table 1). The reproducibility of the intrusion curves increases for the foil samples. The interparticle spacings observed in the powder samples do not occur in the electrode foils, indicating that PTFE is plastically deformed in the fabrication process, filling the voids between the carbon particles.

Figure 10 shows the mercury intrusion curve for the cathode diffusion layer, and Fig. 11 the resulting pore size distributions. The KOH contact angle increased from 97° (SH100) to 118°, which can be attributed to the addition of 37.5% PTFE powder. Structural changes due to these additives are minor, as the characteristic pores appear in both the powder and the electrode sample. The pores left behind by the bicarbonate filler (around 100 μm, see SEM, Fig. 12) are not apparent due to poor resolution of the porosimeter at pressures below 2 p.s.i. (pressure difference between the mercury reservoir and the sample).

Figure 13 shows the intrusion curves for the cathode catalyst layer. The contact angle increases from 101° to 109° due to the addition of 11% PTFE. Comparing the KOH and the mercury intrusion curves, it becomes

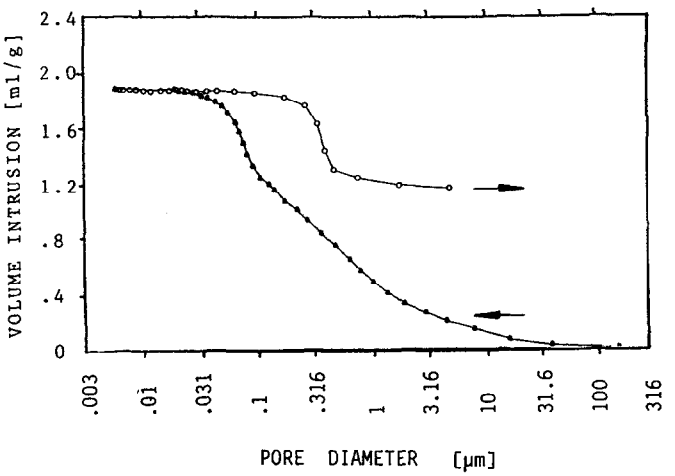

Fig. 10. Mercury volume intrusion and extrusion of a cathode diffusion layer foil.

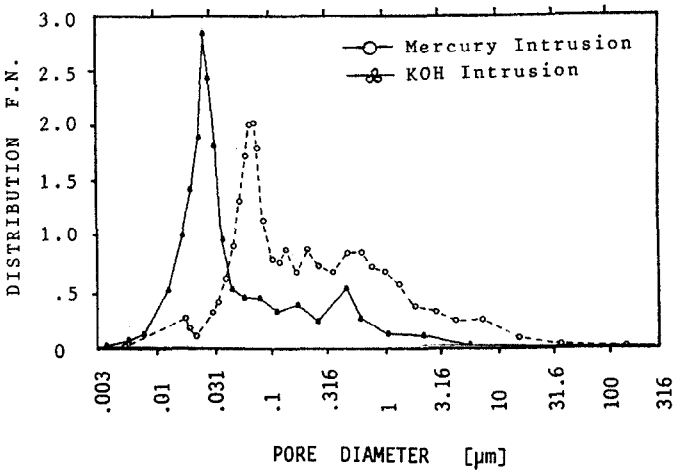

Fig. 11. Pore size distribution for mercury and 12 N KOH intrusion of a cathode diffusion layer foil.

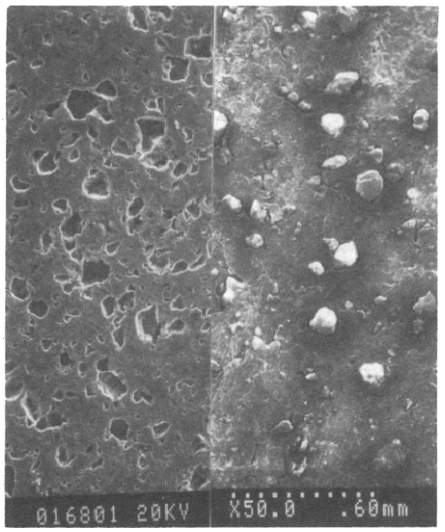

Fig. 12. Scanning electron microscope (SEM) picture of the back side of a cathode diffusion layer foil (left: filler removed; right: filler present).

obvious that the electrolyte wets all but the inside of the carbon particles, assuring a sizeable three layer interface where the electrocatalyst (which primarily is located in discrete particles on the outer surface of the carbon particles, see TEM, Fig. 14), the electrolyte and the reactant gas meet. It is seen that the gas transport in the active layer proceeds through the small, non-wettable pores.

When the partially hydrophobic electrode is contacted by an aqueous solution of KOH, sufficient active sites are contacted to provide a current

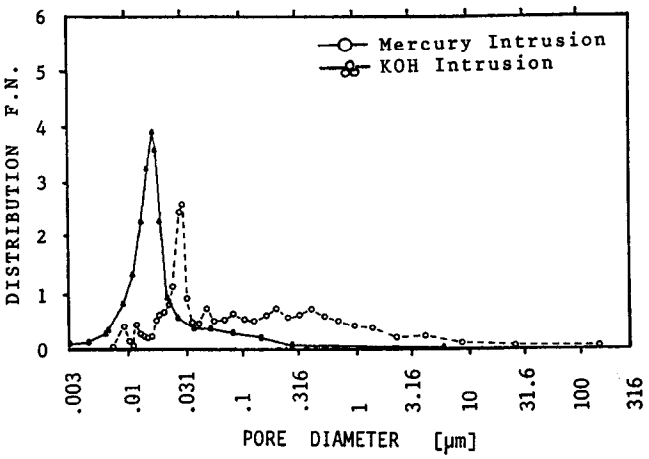

Fig. 13. Pore size distribution for mercury and 12 N KOH intrusion of a cathode catalyst layer foil.

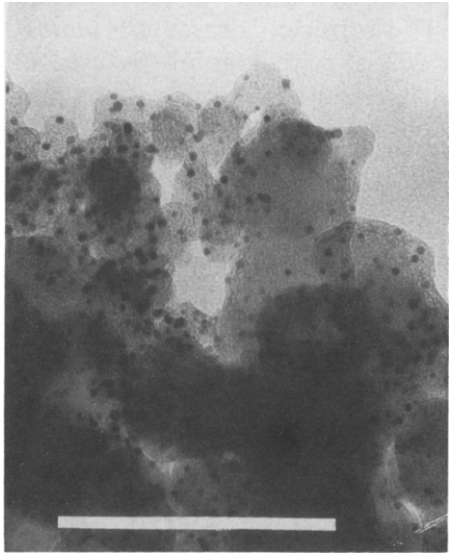

Fig. 14. Transmission electron microscope (TEM) picture of 10% platinum supported on Vulcan XC 72R (Bar = 0.1 μm).

when the reactant gases are fed to the electrode. As a result of this wetting, the three-phase interface region is established very quickly. Cell potentials improve as this wetting-in takes place since more active sites are utilized. This phenomenon is due to the fact that the larger, less wetproofed pores have porous walls which are the terminal endings of all the fine pores ("finger" model). These fine pores, which are not filled with the electrolyte, provide an extensive three-phase region at this junction with the large pores and supply the reactant gas.

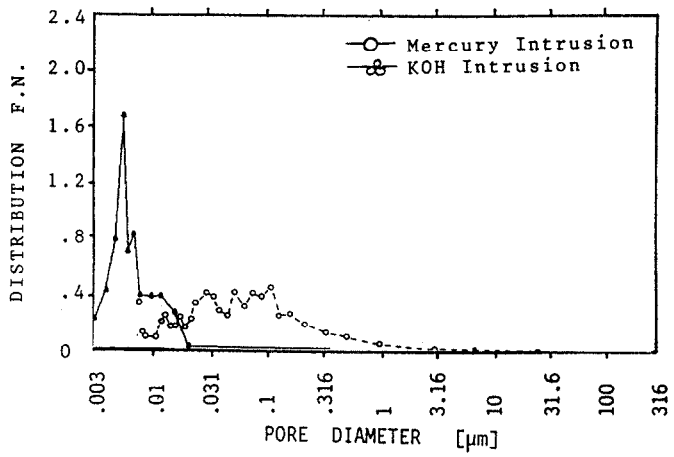

Fig. 15. Pore size distribution for mercury and 12 N KOH intrusion of an anode diffusion layer foil.

Due to the high content of PTFE the hydrogen diffusion layer is substantially denser than the catalyst layer. The intrusion curves are almost identical, as the Black Pearls 2000 carbon mixed with graphite is used in both instances. Comparing the mercury and KOH intrusion curves indicates that all but the very small pores (<0.01 μm) are readily wetted by the electrolyte during fuel cell operation (Fig. 15).

The wetting agent, Triton 100, and film forming agents such as carboxymethylcellulose (CMC), which are added to the Teflon suspension when making the anode active layer, leave residues after the sintering step, greatly reducing the hydrophobicity of the layer. The use of isopropyl alcohol (post catalyzation) also reduces the hydrophobicity of the electrode.

Figure 16 compares the mercury and the KOH intrusion curves for a Union Carbide Corporation T3 electrode. This electrode contains a porous

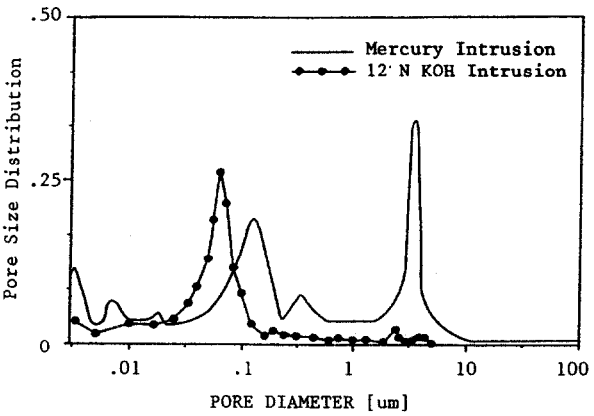

Fig. 16. Pore size distribution for mercury and 12 N KOH intrusion of a Union Carbide T3 electrode.

nickel plaque as current collector facing the electrolyte. The active layer is sandwiched between the diffusion layer and the nickel backing. It can be seen that the porous nickel plaque (3 μm pore diameter) is significantly decreased in intensity, which can be explained by the fact that metals are hydrophilic and almost entirely wetted (flooded) by the electrolyte.

When the PTFE–carbon layers are formed, the carbon particles are brought together in a tighter pack during the rolling and pressing operation. Compacting was not found to appreciably affect the pore structure in the pore diameter range below 1 μm. The use of acetylene black results in a less dense packing compared with other carbon materials, a property also maintained in a PTFE–carbon layer. This factor probably accounts for the superior operating characteristics of electrodes containing Shawinigan SH100 diffusion layers and the fact that these layers can be made up with higher PTFE concentrations. The greater pore diameter of Shawinigan SH100 as compared with, for example, Vulcan XC 72R, accounts for the good gas transport properties. The voltage difference between air and oxygen performance at current densities up to 150 mA cm^{-2} is kept at, or close to, the theoretical value. The high PTFE concentrations significantly improve the hydrophobicity of the layer over the powder alone. The introduction of Shawinigan SH100 into the anode diffusion layer, replacing the Black Pearls 2000 carbon, resulted in reduced electrode weeping as well as improved performance and lifetime.

A reduction in surface area as compared with the surface areas of the components becomes apparent with PTFE-bonded carbon structures. Table 1 lists the surface areas of the different foils, measured using a BET surface area meter, and values calculated using the surface areas of the components. PTFE tends to flow during the rolling (green bonding) and sintering process, covering the carbon surface and partly blocking some pores or totally encapsulating smaller particles. These effects are more noticeable with greater percentages of PTFE. In the electrode fabrication process PTFE is plastically deformed and assumes the shape of the "voids". The effect of greater concentrations of PTFE on the hydrophobicity of pores below 0.1 μm is not significant. In order to wetproof the small pores of the carbon particles it is essential to use a liquid wetproofing agent (*e.g.*, paraffin oil or wax dissolved in petroleum ether, or poly(ethylene) wax dissolved in toluene).This wetproofing step appears to increase the average wetting angle by approx. 5°, primarily by virtue of the increased hydrophobicity of the micropores [27].

Although the active layer is not strongly hydrophobic, it wets in rather slowly. Electron microscopic investigations of the electrolyte penetration of the active layer of gas diffusion electrodes were performed on electrodes operating at a current density of 100 mA cm^{-2} at 65 °C in 12 N KOH. Using XES techniques to trace potassium it has been found that within the first 200 h the electrolyte penetrates about 200 μm into the layer and the electrolyte front reached the diffusion layer in a 400 μm active layer electrode after 500 - 750 h (Figs. 17 - 19).

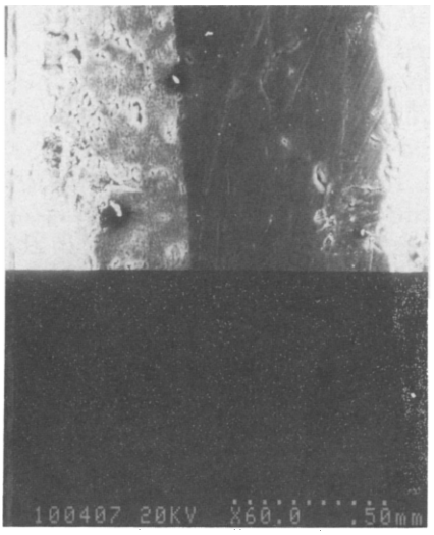

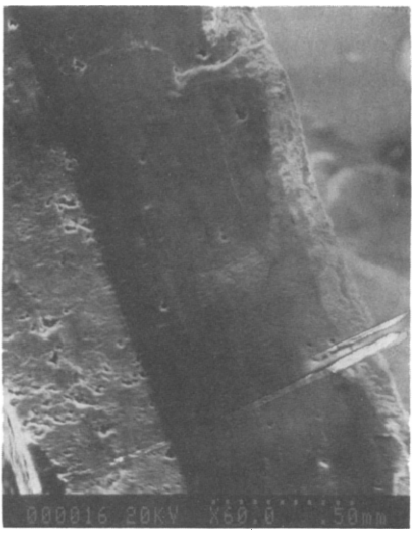

Fig. 17. SEM/XES graph of an air cathode cross section after 1 h operation in 12 N KOH (100 mA cm^{-2}, 65 °C). Tracing element: potassium.

Fig. 18. SEM graph of an air cathode cross section after 217 h operation in 12 N KOH (100 mA cm^{-2}, 65 °C).

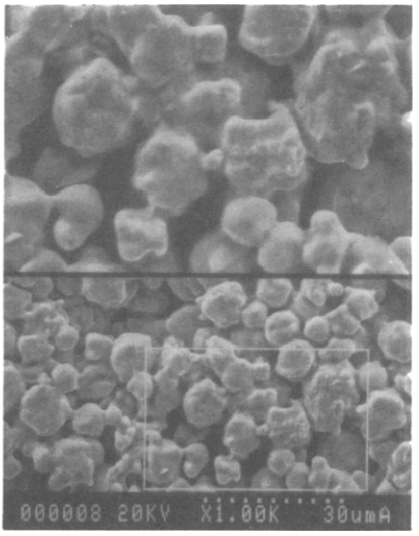

Fig. 19. XES graph of an air cathode cross section after 217 h operation in 12 N KOH (100 mA cm^{-2}, 65 °C). Tracing element: potassium.

Fig. 20. SEM graph of a Union Carbide Corporation porous nickel plaque. The upper section is magnified by the factor 2.

Electrode model

A significant difference exists between the structure of porous metal- and plastic-bonded-carbon gas diffusion electrodes [28]. Figure 20 shows an SEM picture of a Union Carbide porous nickel plaque wetproofed with

PTFE suspension. The 3 μm pores (interparticle spacing) are strongly depressed in the porosimeter curves obtained with KOH (see Fig. 16) indicating that they are filled with KOH prior to the application of intrusion pressure. The metal particles are completely wetted by the electrolyte, low in surface area (below 30 $m^2\ g^{-1}$), and have very little inner surface and porosity. Giner and Hunter describe metal particles forming porous agglomerates which, under working conditions, are flooded with electrolyte [29]. The metal agglomerates are kept together by the PTFE binder which creates hydrophobic gas channels. As current is drawn from the electrode, reactant gas diffuses through the channels, dissolves in the electrolyte-contained agglomerates, and reacts on available sites of catalyst particles.

Carbon particles, however, have a large surface area (50 - 2000 $m^2\ g^{-1}$) and have a pronounced microstructure. The pores of the carbon particles can be free or partially filled with the electrolyte, depending on the interfacial tensions prevailing in the pores [30]. Electron microscopy and intrusion porosimetry analysis of gas diffusion electrodes revealed that the structure of PTFE bonded, multilayer gas diffusion electrodes consists of two components: a primary (macro) structure and a secondary (micro) structure. The pores created by those two structures fulfill several functions in the diffusion and the active layer of gas diffusion electrodes [31].

The primary structure is created by the partial enclosure of the carbon particles by the PTFE. This electrode skeleton can be varied by the use of different particle sizes and shapes of carbons and PTFE, by the electrode fabrication process (pressing, rolling or spraying), by the drying and sintering process, and by the incorporation of filler materials (liquid: *e.g.*, suspension agents, solid: *e.g.*, ammonium bicarbonate). The pore system in the skeleton structure typically exceeds 1 μm. The primary or skeleton structure serves as the current collector, ensuring electronic conductivity and gives the electrode mechanical support [31].

The electrode microstructure (secondary structure) is created by the pore system of the carbon particles. This secondary electrode structure depends on the surface area and the pore structure of the particular carbon used. The secondary pore structure of the carbon is established in the carbon manufacturing process (furnace black: Vulcan XC 72R, acetylene black: Shawinigan SH100, oil flame black: Lampblack, activated carbon: Black Pearls 2000). The choice and pretreatment of carbon materials for use in gas diffusion electrodes is therefore of prime importance [6]. Carbon pretreatment methods used (*e.g.*, gas activation) not only improve the chemical stability of the carbon, but also significantly modify the micropore structure [27].

Gas transport is ensured mainly by the secondary pore structure. In the *diffusion layer*, however, no electrolyte is present and therefore both the primary (large pores are liquid free) and the secondary pore structure are responsible for the transport of fuel and reactants. In the *active layer* the gas transport proceeds almost entirely through the small pores as the macropores are filled with the electrolyte.

The three phase interface is created in the transition region between the two pore structures in the outer regions of the carbon particles. TEM/XES analysis of carbon before, and after, use in fuel cell electrodes revealed that the catalyst is located in discrete particles (15 - 100 Å) in the outer surface of the carbon particles.

It appears that in the *active layer* the carbon particles are immersed in electrolyte and the inside carbon particles (microstructure) provide for gas transport. The three phase interface, where fuel, electrolyte, and electrocatalyst meet, is created in the outer region of the carbon particles. The pores in the outer carbon shell are covered by a thin electrolyte film, wetting the electrocatalyst particles. A gas–electrolyte equilibrium is maintained, sustaining electrolyte and providing fuel to the reaction sites. The carbon particles are arranged in a "tight bed" and gas transport proceeds through the carbon pore system, maintained by capillary forces and the hydrophobic binder, while the (bigger) vacancies created by the "packed spheres" serve as an electrolyte reservoir. The "tight bed" carbon structure provides a means of electron and gas transport. The vacancies created by the carbon/PTFE structure ensure ionic transport.

4. Conclusion

The structural parameters of electrodes and electrode materials strongly influence the performance characteristics of PTFE bonded, porous gas diffusion electrodes. SEM, TEM, and intrusion porosimetery studies on electrode components and electrode foils revealed that electrodes are composed of a primary and a secondary electrode structure. Electrochemical performance as well as degradation mechanisms can be related to structural parameters. Comparing intrusion porosimetry data obtained with mercury and electrolyte (*e.g.*, 12 N KOH) as intrusion liquids has been used to reveal individual functions of structural parameters. The wetting angle for the electrolyte is substantially lower than for mercury, resulting in penetration of the same pore at a significantly reduced pressure. Using electrolyte penetration, transitional and micropores can therefore be determined with greater accuracy as the porosimeter experiences a noticeable blank intrusion at higher intrusion pressures. Macropores can be determined with greater accuracy using mercury as the intrusion liquid. On powder samples pores created by interparticle spaces can be eliminated using electrolyte intrusion.

Measurements of this kind contributed significantly to the selection of electrode materials and design optimization of the gas diffusion electrodes. Acetylene black was determined to be the material of choice for the diffusion layer and Black Pearls 2000, mixed with graphite, for the electrocatalyst layer of fuel cell electrodes. As no electrolyte is present in the *diffusion layer* the gas transport can proceed through both the micro and macropores. In the *active layer* the macropores were found to contain the electrolyte and provide for the ionic transport, whereas the gas transport

proceeds through the micropores of the carbon particles. The electrochemistry proceeds in the boundary between the micro and macrostructure where a three zone interface between electrocatalyst supported on carbon, electrolyte, and gas, is created. Reactant gas dissolves in the electrolyte and diffuses to the electrocatalyst where it reacts when power is drawn from the cell.

It is conceivable that measurements of this kind on electrodes before, during, and after operation in fuel cells will reveal information regarding the nature and extent of electrolyte penetration and structural degradation. Intrusion porosimetry at different (fuel cell) operating temperatures will greatly enhance the understanding of electrolyte–electrode interaction.

Acknowledgements

This work was funded by the Ontario Ministry of Energy (OMENG) and the Austrian Funds to Support Science and Technology. Permission given by Battery Technologies Inc. to release the paper for publication is appreciated.

References

1 M. B. Clark, W. G. Darland and K. V. Kordesch, *18th Annu. Power Sources Conf., Atlantic City, NJ, 1964*, The Electrochemical Society, Pennington, NJ, pp. 11 - 14.
2 K. V. Kordesch, *Fuel Cells*, Springer, New York, 1984.
3 G. V. Elmore and H. A. Tanner, *U.S. Pat. 3,419,900* (1968), applied for March, 1960.
4 C. L. Mantell, *Carbon and Graphite Handbook*, Interscience, New York, 1968.
5 P. L. Walker, Jr. and P. A Thrower (eds.), *Chemistry and Physics of Carbon*, Vol. 1 - 16, Marcel Dekker, New York, 1965 - 1981.
6 K. V. Kordesch, Survey of carbon and its role in phosphoric acid fuel cells, Final Rep., 1979, *Brookhaven Nat. Lab., Contract BNL 51418 (NTIS)*.
7 Yvan Schwob, Acetylene black, manufacture, properties, applications, in *Chemistry and Physics of Carbon*, Vol. 15, Marcel Decker, New York.
8 K. Tomantschger, F. McClusky, A. Reid, L. Oporto and K. Kordesch, Performance evaluation of the Institute for Hydrogen Systems porous gas diffusion electrodes, *Institute for Hydrogen Systems Rep.*, 1986, Institute for Hydrogen Systems, Mississauga, Ont., Canada.
9 D. Rivin, *Rubber Chem. Technol., 44* (1971) 307 - 343.
10 *Special Blacks Tech. Service Rep. S-38*, Black Pearls 2000, Superconductive Carbon Black, Cabot Corporation, 125 High Street, Boston, MA 02110, U.S.A.
11 K. Tomantschger, J. Gsellmann, M. Hanson and K. Kordesch, *The Electrochemical Society Spring Meeting, Philadelphia, PA, May 10 - 15, 1987, Ext. Abstr. No. 315*, pp. 461 - 462.
12 S. T. Narsavage, R. W. Vine and R. C. Emanuelson, *U.S. Pat. 3,859,138* (1975).
13 R. W. Froberg, *U.S. Pat. 3,944,686* (1976).
14 L. G. Christner, D. C. Nagel and P. R. Watson, *U.S. Pat. 4,115,528* (1978).
15 D. A. Schulz, *U.S. Pat. 3,960,601* (1974).
16 W. T. Thomson, *Philos. Mag., 42* (1871) 448.
17 M. M. Dubinin, *Zh. Fiz. Khim., 34* (1960) 959.

18 T. Van der Plas, in B. G. Linsen (ed.), *Physical and Chemical Aspects of Adsorbents and Catalysts*, Academic Press, New York, 1970, Ch. 9.
19 E. W. Washburn, *Proc. Nat. Acad. Sci.*, 7 (1921) 115.
20 L. C. Ritter and A. L. Drake, *Ind. Eng. Chem., Anal. Ed., 782* (1945) 17.
21 S. Lowell, *Introduction to Powder Surface Area*, Wiley, New York, 1979, pp. 182 - 184.
22 PMI Intrusion Porosimeter Model 200-8101, *Porous Materials Inc. Product Information, 1985.*
23 K. Tomantschger, J. Gsellmann, M. Hanson and K. Kordesch, *The Electrochemical Society Spring Meeting, Philadelphia, PA, May 10 - 15, 1987, Ext. Abstr. No. 414*, pp. 459 - 460.
24 F. A. Heckman and D. F. Harling, *Rubber Chem. Technol., 39* Pt. I (1966) 1 - 13.
25 K. Tomantschger and L. Oporto, Fabrication procedures for IHS gas diffusion electrodes, *Institute for Hydrogen Systems Propr. Rep.*, 1985, Institute for Hydrogen Systems, Mississauga, Ont., Canada.
26 K. Tomantschger, F. McClusky, L. Oporto, A. Reid and K. Kordesch, *J. Power Sources, 18* (1986) 317 - 335.
27 R. J. Elbert, The characterization of fuel cell electrodes and electrode materials, *Propr. Res. Rep. URS-247*, Union Carbide Corp., (photos released 1977).
28 J. Giner, J. M. Perry, S. Smith and M. Turchan, *J. Electrochem. Soc., 116* (1969) 1692 - 1696.
29 J. Giner and C. Hunter, *J. Electrochem. Soc., 116* (1969) 1124 - 1130.
30 K. Kordesch, J. Gsellmann, S. Jahangir and M. Schautz, in H. Maru (ed.), *Proc. Symp. on Porous Electrodes: Theory and Practice, Proc. Electrochem. Soc. 84-8* (1984) 163 - 190.
31 K. Tomantschger, F. McClusky, A. Reid, L. Oporto and K. Kordesch, in D.-T. Chin (ed.), *Proc. Symp. on Load Leveling and Energy Conservation in Industrial Processes, Proc. Electrochem. Soc., 86-10* (1986) 113 - 132.